

Experimental and Numerical Analysis on Impacts of Significant Factors on Carbon Dioxide Absorption Efficiency in the Carbon Solidification Process

Haibin Wang^{*1,2}, Peilin Zhou² and Zhongcheng Wang²

1- Department of Naval Architecture, Ocean and Marine Engineering, University of Strathclyde, Glasgow, UK

2- Merchant Marine College, Shanghai Maritime University, China

Abstract

Onboard carbon capture and storage is an excellent solution to reduce the greenhouse gas emissions from shipping. This paper focuses on the absorption process and CO₂ gas flow rate, the geometry of absorption tank and the concentration of absorption solution are key factors affecting the absorption efficiency. This paper will illustrate the experimental results of the impacts of these factors on the CO₂ absorption efficiency. Meanwhile, results from CFD simulations of effects of the key factors on CO₂ absorption rates will be presented in this paper. Pressure distributions, solution concentration and velocity of CO₂ gas and solution are derived from the simulations. The results of the simulations provide fundamentals and insight understanding of the design of a proto-type demonstration system onboard a case ship. In addition to the key factors, the effect of atmosphere temperature was simulated and analyzed. Comparisons between the experiment and simulation have been conducted and the results have shown a good agreement. Optimized values of the factors are obtained from the comparisons and analyses. The numerical simulations of temperature effects on CO₂ absorption rate and optimized temperature for the absorption process are also presented in the paper.

*Corresponding author at: Department of Naval Architecture and Marine Engineering, Henry Dyer Building, 100 Montrose Street, University of Strathclyde, G4 0LZ, Glasgow, UK. Tel.: +44 (0)141 548 3344; fax: +44 (0)141 552 2879.

E-mail address: haibin.wang.100@strath.ac.uk

Keywords: Emission reduction; chemical absorption; two-phase flow simulation.

-- Insert Nomenclature here --

1. Introduction

Greenhouse gases (GHG) are the main reason for climate change. It leads to many disasters to our human beings. Melting glaciers, rising sea levels and extinction of endangered species keep impacting our living conditions on the earth. These phenomena are resulting from the temperature rising continuously due to the thermal insulation effect of GHG. The heat received by earth cannot be rapidly released into the space and resulting in global warming. The GHG emission has to be reduced in order to guarantee the safety of our planet in the future. There are many kinds of GHG existing, such as carbon dioxide (CO₂), methane (CH₄), nitrous oxide (N₂O) and fluorinated gases (F-gases). Among all the GHG, presented in Figure 1, CO₂ is the most influential one which contributes 76.7% of the anthropogenic GHG emissions to atmosphere (IPCC, 2007). Nowadays, there are a large number of research projects focusing on different methods to mitigate the effect of global warming by reducing CO₂ gas emission. One of the most effective and popular methods is the carbon capture and storage (CCS). CCS is considered to be an effective way to mitigate and even eliminate the global warming effect through capturing the CO₂ emission and storing them underground for Enhanced Oil Recovery (EOR) or in deep seas (World Resources Institute, 2008). However, CCS system currently is only applied on onshore power plants and some industrial processes. There are few marine applications. About 938 million tons of CO₂ emission is estimated from shipping and 796 million tons are contributed by international shipping in 2012. (Third IMO GHG study 2014, 2014) 20% reduction of carbon emission from ships is also set up as a global target to be achieved in 2020 by United Nations. (Shipping, World Trade and the Reduction of CO₂ Emissions, 2014) Although it is about 2.2% of the global CO₂ emissions, International Maritime Organization (IMO) has already taken actions to reduce GHG

emissions from ships, such as EEDI, EEOI and SEEMP, aiming to increasing the energy efficiency of ships. (MARPOL Annex VI, Chapter IV, 2011)

By the end of the 2012, there have been 14 active CCS industrial projects on shore. (Global CCS Institute 2012, 2012) Boundary Dam Integrated Carbon Capture and Sequestration Demonstration Project is an active CCS project launched in 2014 in Canada. The target is on the power station. An amine based post-combustion capture method is applied for capture. The transport type is using pipeline and EOR is selected for carbon storage. (Boundary Dam Integrated Carbon Capture and Storage Demonstration Project, 2014) Gorgon Carbon Dioxide Injection Project is an Australian project under execute and will be in operated in 2016. The target is on natural gas processing and this CCS project will apply pre-combustion capture method (natural gas processing), pipeline and EOR. (Gorgon Carbon Dioxide Injection Project, 2015) FutureGen 2.0 Project is an under defined CCS project and will apply oxy-fuel combustion capture method on power station in USA. Compression method will be applied for separation. Pipeline and dedicated geological storage will be utilized for CO₂ transportation and storage. (FutureGen 2.0 Project, 2013)

For Marine applications, Det Norske Veritas (DNV GL) and Process Systems Enterprise Ltd have launched projects on maritime CCS applications and a report has indicated that, with CCS on ship, CO₂ emission can be reduced by 65% (DNV and PSE report on ship carbon capture & storage, 2013). It also proves that CCS is not only an excellent supplement of energy improvement methods but also an effective CO₂ emission reduction method. From previous work of the authors, it indicates the feasibility of proposed CCS method to reduce marine CO₂ emission by separating and storing them in a solid form on ships. Case study from previous work also have illustrated the proposed solidification processes is more cost effective than the traditional liquefaction method for CO₂ storage onboard. (Peilin and Haibin, 2013)

In order to design a reasonable and feasible CFD model, several literatures are reviewed. Horvath and his research group have successfully modelled and simulated a cuboid bubble column using the VOF model. VOF model is suitable to present immiscible phase interaction and the computation cost is quite small. Their results are close to

the experiment data. (Horvath et al., 2009) The investigation from Mohammad I. and Mohammad A. K. tests both mixture and Eulerian approaches on a bubble column reactor at unsteady state conditions and low gas flow rates. The results from simulation have a good consistency with experiment data. It also indicates similar outputs are derived from mixture and Eulerian model but the Eulerian model has a better convergence and stability. (Mohammad, I. and Mohammad, A.K., 2011) Asendrych and his colleagues applied a two-fluid Eulerian model for an amine based carbon capture system. A 2D axisymmetric CFD model was designed and analyzed. The results illustrate the ratio of solution to gas has a significant impact on efficiency. They also achieved a good agreement of numerical results and experiment data. (Asendrych et al., 2013)

This paper presents the experiment conducted to estimate the effects of various factors on the CO₂ absorption rate. Numerical simulations of the absorption process are also illustrated. An Eulerian model will be selected and a 2D model will be applied. The comparisons of experiment results with that of simulation are also presented, leading to optimized operational factors for CO₂ absorption. The numerical simulations will provide fundamentals of the design of a proto-type demonstration system on ships.

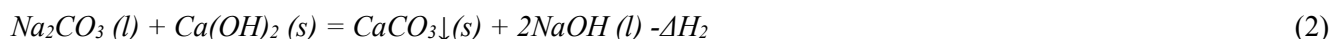
-- Insert Figure 1 here --

Figure 1 Contributions of different GHG gases to global emissions

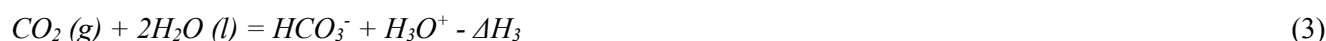
2. Carbon solidification processes

Carbon solidification processes only deal with part of exhaust gases from marine engines as the target is to comply with various regional and international CO₂ emission regulations. Part of the exhaust gas from the funnel is firstly bypassed into a separation system to obtain high purity CO₂ gas. Since it is not attached to main engine, the impact of this system on engine efficiency is very much slight. There are many different methods available to achieve the separation so this paper will focus on the absorption processes dealing with concentrated CO₂ gas. The concentrated CO₂ gas after separation is fed into a reaction tank which contains alkaline solution. Following the absorption of CO₂ by the alkaline solution, calcium oxide (CaO) is added to solidify the CO₃²⁻ ions from the

solution. The chemical reaction processes are presented below by [Eqs. 1](#) and [Eqs. 2](#) (Pflug et al., 1957; Mahmoudkhani and Keith, 2009):



There are two intermediate reactions containing in the above processes shown in [Eqs. 3](#) and [Eqs. 4](#) (Chambers and Holliday, 1975; Hessabi, 2009):



Sodium hydroxide (NaOH) solution is selected as the absorbent because it naturally reacts with acid gas (CO₂, SO₂ and NO₂). After sodium carbonate (Na₂CO₃) is generated, CO₂ is captured in the form of CO₃²⁻ ions in solution. After adding in CaO, it firstly reacts with water to generate calcium hydroxide (Ca(OH)₂). When Ca²⁺ meets with CO₃²⁻ in the solution, sediment calcium carbonate (CaCO₃) is produced. The sediments are separated from the solution and then dried for storage on ship. The sediment will be discharged off ship at end of a voyage in port. Calcium carbonate can be traded to medical industry as calcium supplement or building industry as primary substance of building materials. NaOH solution is regenerated during the precipitation ([Eqs. 2](#)) and can be reused as absorbent in the process in [Eqs. 1](#). In this paper, only the absorption process is analyzed and further consideration on separation and solidification processes will be made in future research works.

This project is a very much forefront idea to apply chemical method on ship for the purpose of carbon emission reduction. Currently, there is no project providing similar comparisons between chemical method and liquefaction method for ships. It is because that not only the energy and chemical cost but also the transportation penalty of the vessel should be considered. Our previous work (Peilin and Haibin, 2013) has a comprehensive consideration on these costs for both methods and the results are presented in that paper as well

3. Methodology of simulation

Chemical process comprises two main components: species transportation and multiphase flow. To simulate a chemical process with CFD tools, both components should be considered. Species transportation is considered in the numerical simulation by transferring masses, energy and momentum of reactants into products. Multiphase flow is simulated as bubble column effects due to the mixing of liquid and gas of reactants. CO₂ and air are in a gas phase and NaOH and Na₂CO₃ solutions are in liquid forms.

ANSYS Fluent solves conservation equations for chemical species by predicting the local mass fraction of each species, through the solution of a convection-diffusion equation for specified species (ANSYS Fluent theory guide 14.5, 2012) as shown in the following:

$$\frac{\partial}{\partial t}(\rho Y_i) + \nabla \cdot (\rho \vec{v} Y_i) = -\nabla \cdot \vec{J}_i + R_i + S_i \quad (5)$$

where Y_i is the local mass fraction of each species. R_i is the net rate of production of species i by chemical reaction and S_i is the rate of creation from the dispersed phase and sources. J_i is the mass diffusion flux. \vec{v} is the overall velocity vector (m/s). t represents time and ρ is the density of species.

For an Eulerian multiphase model, the concept of phasic volume fractions is introduced and the volume of one phase can be defined as:

$$V = \int_V a dV \quad (6)$$

where a is the volume fraction of phases.

The continuity equation of phase q (for fluid-fluid mass exchange) is:

$$\frac{\partial}{\partial t}(a_q \rho_q) + \nabla \cdot (a_q \rho_q \vec{v}_q) = \sum_{r=1}^n \dot{m}_{r \rightarrow q} - \sum_{r=1}^n \dot{m}_{q \rightarrow r} \quad (7)$$

where \vec{v}_q is the velocity of phase q; \dot{m}_{pq} is the mass transferred from the phase p to q and \dot{m}_{qp} is the mass transferred from phase q to phase p.

The energy conservation equation in Eulerian model is:

$$\frac{\partial}{\partial t}(a_q \rho_q h_q) + \nabla \cdot (a_q \rho_q \vec{u}_q h_q) = a_q \frac{\partial p}{\partial t} + \tau_q \cdot \nabla \vec{u}_q - \nabla \cdot \vec{q}_q + S_q + \sum_{p=1}^n (Q_{pq} + \dot{m}_{pq} h_{pq} - \dot{m}_{qp} h_{qp}) \quad (8)$$

where h_q is the specific enthalpy of the q^{th} phase; \vec{q}_q is the heat flux, S_q is a source term that includes sources of enthalpy, such as from chemical reaction; Q_{pq} is the intensity of heat exchange between p^{th} and q^{th} phases, and h_{pq} is the interphase enthalpy (for example, the enthalpy of the vapor at the temperature of the droplets, in the case of evaporation). The heat exchange between phases must comply with the local balance conditions $Q_{pq} = -Q_{qp}$ and $Q_{qq} = 0$.

The conservation of momentum for a fluid phase is:

$$\frac{\partial}{\partial t}(a_q \rho_q \vec{v}_q) + \nabla \cdot (a_q \rho_q \vec{v}_q \vec{v}_q) = -a_q \nabla p + \nabla \cdot \tau_q + a_q \rho_q \vec{g} + \sum_{p=1}^n (K_{pq} (\vec{v}_p - \vec{v}_q) + \dot{m}_{pq} \vec{v}_p - \dot{m}_{qp} \vec{v}_q) + \vec{F}_{lift,q} + \vec{F}_{wl,q} + \vec{F}_{vm,q} + \vec{F}_{td,q} \quad (9)$$

where ρ is the density; p is the pressure shared by all phases; g is gravitational acceleration and K is the momentum exchange coefficient between fluid phases. \vec{F}_q is an external body force (arise from interaction with the dispersed phase), $\vec{F}_{lift,q}$ is a lift force (lift force impacts secondary phase due to velocity gradients in the primary phase flow field), $\vec{F}_{wl,q}$ is wall lubrication force (secondary phase bubbles are subjected to wall lubrication force which tend to bounce bubbles away from walls), $\vec{F}_{vm,q}$ is a virtual mass force (it occurs when a secondary phase accelerates relative to the primary phase), $\vec{F}_{td,q}$ is a turbulent dispersion force (this acts as a turbulent diffusion in dispersed flows and for turbulent flow only).

$\bar{\tau}$ is the stress-strain tensor of q^{th} phase:

$$\bar{\tau}_q = \alpha_q \mu_q (\nabla \vec{v}_q + \nabla \vec{v}_q^T) + \alpha_q \left(\lambda_q - \frac{2}{3} \mu_q \right) \nabla \cdot \vec{v}_q I \quad (10)$$

where μ_q and λ_q are the shear and bulk viscosity of phase q and I is the unit tensor.

\vec{v}_{pq} is the interphase velocity, defined as follows. If $r_{pq} > 0$ (that is, phase p mass is being transferred to phase q),

$\vec{v}_{pq} = \vec{v}_p$; If $r_{pq} < 0$ (that is, phase q mass is being transferred to phase p), $\vec{v}_{pq} = \vec{v}_q$. If $r_{pq} = 0$, then $\vec{v}_{pq} = \vec{v}_q$; If

$r_{pq} < 0$, $\vec{v}_{qp} = \vec{v}_p$.

Reaction rate, r , between phases can be derived by following equation:

$$r = k(T)[A]^m[B]^n \quad (11)$$

Where $k(T)$ is the reaction rate constant that depends on temperature, $[A]$ and $[B]$ are the concentrations of substances A and B in moles per volume of solution (assuming the reaction is taking place throughout the volume of the solution) and exponents m and n are partial orders of reaction which depend on reaction mechanism.

Reaction rate constant, k , is estimated by using Arrhenius expression:

$$k = AT^\beta e^{-Ea/RT} \quad (12)$$

where A is the pre-exponential factor; T is the temperature of reactants; β is the temperature exponent; Ea is the activation energy for reaction and R is the universal gas constant.

The surface tension is involved in modelling of the bubbling effect:

$$\Delta p = \frac{2\sigma}{R} \quad (13)$$

where Δp is the pressures difference between two sides of the surface; σ is the surface tension coefficient; and R is the radius of bubbles.

Wall adhesion is also considered for bubbling effect and the surface normal at the live cell next to the wall is:

$$\hat{n} = \hat{n}_w \cos \theta_w + \hat{t}_w \sin \theta_w \quad (14)$$

where \hat{n}_w and \hat{t}_w are the unit vectors normal and tangential to the wall; θ_w is the tangent angle of the gas bubbles or liquid droplets to the wall as indicated in Figure 2. Jump adhesion is usually applied on porous jump boundary condition so this model will not include jump adhesion as no porous jump boundary condition is applied.

-- Insert Figure 2 here --

Figure 2 Demonstration of contact angle between gas-solution surface and wall.

4. Experiment rig and CFD simulations

4.1. Experiment rig setup

Based on the principles of absorption and solidification processes introduced above, two steps of experiment are designed: chemical absorption and precipitation, and physical filtration. Figure 3 is the experiment rig used for absorption processes and the schematic diagram. High purity CO₂ from a gas bottle is fed into a measuring cylinder as a reaction tank which contains prepared NaOH solution. The gas goes through a gas regulator and a flow meter to adjust the gas pressure and input flow rate. Fitted with a pipe, a gas diffuser is installed to generate gas bubbles in order to increase the contact area between gas and solution. The mass changes of CO₂ bottle and measuring cylinder are monitored and measured by two scales for the measurements of CO₂ gas supplied from gas bottle and absorbed in solution.

-- Insert Figure 3A here --

A

-- Insert Figure 3B here --

B

Figure 3 A: experiment rigs; B: schematic chart of absorption process

According to Figure 3, there are two scales involved in the measurements: one is measuring the CO₂ bottle and the other one is measuring the reaction tank (measuring cylinder with solution). There is also another scale measuring chemical raw materials which is not included in the figure. The types, ranges and accuracy of these scales are presented in Table 1. The weight of full CO₂ tank is over 18000 g and the initial weight of reaction tank (with designed quantity of solution) is over 1000g. The weight of each chemical material is no more than 170 g for this lab-scale experiment. Therefore these scales are accuracy enough for measurements based on this table.

Table 1 Details of scales used in experiment measurement.

-- Insert Table 1 here --

4.2. Assumptions, modelling and CFD simulations

Before modelling and simulation, a range of assumptions is essential to be applied in order to simplify the problem and model geometry:

1. Temperature, pressure and gravitational acceleration of surrounding environment are set respectively as 298K, 101325 Pa and 9.81 m/s².
2. The measuring cylinder is simplified to a 2 dimensional model which is shown in Figure 4.
3. For the gas bubble column simulation, the diffuser is simplified as ten separated inlets at the bottom of the measuring cylinder to avoid unstructured grid.
4. The gas fed in is assumed to be ideal gas. The density of fluids and gases mixture material is derived applying volume weight mixing law.
5. The gas bubbles have a minimum diameter of 1×10^{-5} meters.
6. An extension of measuring cylinder is applied to avoid the impacts of backflow on absorption reaction.
7. Each chemical solution is treated as a unified hydrated compound in the simulation.

The geometry is modelled and meshed with Gambit. The system is simplified as a column constituted by solid walls with ten gas inlets at the bottom and one outlet on the top. The geometry of the model uses the actual dimensions of the experiment rig, i.e. the height of solution in the column is 0.3 m and the width of the column is 0.06 m. The structure grid is applied with a minimum length of 5×10^{-4} m and there are 108,000 cells in this model. Considering the shape of 2 dimensional cylinders is a rectangular, the structure meshing in CFD is selected (Jiyuan et al., 2013). The gas flow rate in experiment is 3 l/min and correspondingly the gas input flow rate in the simulation is 1.90×10^{-3} kg/s.

The simulation of absorption reaction is conducted based on Fluent, including both the chemical reaction and bubble column simulations. Since the simulation involves a chemical reaction and a two-phase flow at the same time, the Eulerian model is selected. It is because Eulerian model is compatible with multiphase reaction simulation. Another reason is that it can also simulate the process very much approaching to practical hydrodynamics phenomenon (Asendrych et al., 2013).

CFD for a two phase flow with chemical reaction is very much time consuming. For example, one of the absorption experiments in real life took about 400s. However, in numerical simulation, with a time step of 5×10^{-3} s, the total time steps are 80,000. With the use of High Performance Computer from ARCHIE-WeSt, each step of the simulation in the real time takes about 2s with 4 cores. Hence, for each case, it costs 45 hours in real life and about 178 CPU-hours computing time on HPC.

-- Insert Figure 4 here --

Figure 4 Modeling and meshing of experiment rigs

5. Results and discussions

This section will demonstrate the results of numerical simulations of the reaction process. Critical parameters will be analyzed which will be used for further research on designing of a proto-type demonstration system onboard of

a case ship. The second half of this section will present the comparisons and discussions of the experiment data and numerical simulation results.

5.1. Demonstrations of simulation

Figure 5 presents the CO₂ bubbles flow in the fluid domain, indicating the volume fraction contours of solution at t = 0s and t = 3s. It is a 3 seconds simulation of bubbling effect because the project is majorly focusing on reaction part and too high computing intensity is another reason. The bubbling effect is reasonable as there is a range of different diameter of bubbles. Since the chemical reaction is not taken into account, the height of solution is increased only because gas and liquid phases are immiscible. Both gas phase and liquid phase take volumes in the reaction tank.

-- Insert Figure 5 here --

Figure 5 Bubble flow phenomenon under contours of solutions volume fraction (A: contours graph at t = 0s; B: contours graph at t = 3s.)

Since the simulation of combining chemical reaction with bubbling effect, further simplification of inlet is applied due to computing intense and time consuming. Ten separated inlet boundaries are merged as one integrated gas inlet. With the integrated inlet, the minimum size of mesh is increased resulting reduce of number of mesh of reaction tank model.

Mass fraction of Na₂CO₃ in the solution phase is monitored during the simulation. In the experiment, the final mass fraction of Na₂CO₃ is 76.81%, so that the simulation will be terminated while the mass fraction reaches the same value. According to the Arrhenius expression in [Eqs. 12](#), the reaction rate constant (k) is determined by three factors, i.e. pre-exponent factor, activation energy and temperature, thus, the reaction in CFD simulation is dominated by these factors as well. The simulation can be optimized by controlling these factors. Figure 6A presents the mass fraction of Na₂CO₃ changing over time for both the simulation and experiment. It indicates that the maximum difference between the simulation and experiment is 5.61%. Since these two curves are well

matched, the fundamental factors in this simulation are accepted and will be applied in further simulations. Figure 6B presents the volume fraction of solutions at $t = 400$ s. It illustrates the distribution of gas and solution and the gas moving path while the reaction is processing.

-- Insert Figure 6A here --

A

-- Insert Figure 6B here --

B

Figure 6 A: Comparison of Na_2CO_3 mass fractions over time between experiment and simulation results; B: Volume fraction of solutions at $t = 400$ s.

5.1.1. Concentration of solution

As the absorption progresses, the solution of NaOH reacts with CO_2 and generates Na_2CO_3 . The CO_2 absorbed at different time can be indicated by the mass of the solution. The increment of the mass of the solution represents the quantity of CO_2 being absorbed. Since all the CO_2 trapped in the solution will be in the form of ion CO_3^{2-} , the mass fraction of the Na_2CO_3 solution can also indicates the amount of CO_2 gas absorbed. The mass concentration of Na_2CO_3 at different time is presented in Figure 7. In this figure, the color code stands the mass fraction of Na_2CO_3 in the solution. The color of solution turning from blue to red means the mass fraction of Na_2CO_3 increases from 0 to 100%. It illustrates the increase of the Na_2CO_3 mass fraction during the process of CO_2 absorption. A reasonable explanation of these dots is that the air from the atmosphere is get into the solution and affected the concentration of CO_2 , resulting reduction of reaction rate. With reduced reaction rate, Na_2CO_3 generated will be slowed down so that the concentrations of Na_2CO_3 in these regions are lower than others

-- Insert Figure 7 here --

Figure 7 Concentration contours of Na_2CO_3 in solution over flow time (at 0s, 100s, 200s, 300s and 400s).

5.1.2. Velocity of gas and solution

Once CO₂ is released from the diffuser to the solution, the gas will go upward to the free surface of the solution.

The path and the velocity of the gas at different flow times are presented in

Figure 8. It illustrates the gas velocity in the central area is the highest. It is because the viscous force between two phases drags the gas downward from moving up. According to Figure 9, the reactive force also drives the solution circulating in the fluid region. The velocity of the solution in the center is the highest because part of the solution in the center is mixed and moving with the gas.

-- Insert Figure 8 here --

Figure 8 Gas velocity contours over flow time (at 50s, 225s and 400s).

-- Insert Figure 9 here --

Figure 9 Solution velocity contours over flow time (at 50s, 225s and 400s).

5.2. Comparisons of results from numerical simulation and experiment

5.2.1. Impact of initial NaOH concentration on gas absorption rate

The effect of initial concentration of the NaOH solution on the gas absorption rate is examined under experiment scale. Gas from CO₂ bottle is fed into the NaOH solutions of several different concentrations. The results of the experiment are shown in Figure 10, compared with the simulation results. The comparison of the results indicates the simulation and experiment has a good agreement, including a similar tendency of gas absorption rate change over different initial concentrations of NaOH solution. The absorption rate of gas varies with the NaOH concentration. It reaches to the maximum value when the initial NaOH concentration is 15%.

-- Insert Figure 10 here --

Figure 10 Comparison of experimental and simulated gas absorption rate with different concentrations of NaOH solution

With the same reaction tank geometry, there are two factors dominating the reaction rate between the gas and solution, i.e. the NaOH solution concentration and the contact area between the two phases. At a low concentration of NaOH, the gas absorption rate is increased as the concentration of solution is increased. While the concentration of the solution increases the density of the solution is also increased. Usually, a high density of solution will lead to a high pressure to gas bubbles. According to [Eqs. 13](#), the bubble size will be decreased while the solution pressure grows. At about 15% NaOH concentration, the gas bubble size is decreased to a critical value at which a further increase in the concentration of solution will lead to a decrease in the gas absorption rate.

-- Insert Figure 11 here --

Figure 11 Na₂CO₃ concentrations over time for different concentration of NaOH solutions.

Figure 11 indicates CFD simulation results in the mass fraction of Na₂CO₃ changes over flow time under different solutions. When the initial concentration of NaOH solution is 5%, it only takes about 450s to achieve 100% of reaction (full reaction of NaOH solute). With the increase of NaOH concentration, more NaOH solute is available in the solution so the time taken to reach full reaction becomes longer. Although the time spent for full reaction is lowest when the concentration of NaOH solution is 5%, the actual gas absorbed is the least compared with other cases. To select the optimized initial concentration of NaOH solution, the NaOH solute reacted per second is considered. It presents the reaction rate with various concentration of NaOH solution. It can be derived with following equations:

$$A = C/t \tag{15}$$

where, A is mass of NaOH solute reacted per second in unit volume; C is the mass of NaOH solute in unit volume of solution and t is the total time for full reaction.

$$C = I \times \rho \times c \tag{15-1}$$

where, ρ is the density of NaOH solution and c is the mass fraction of NaOH in the solution. Quantity 1 presents unit volume of NaOH solution. Unit volume is used to simplify the calculation as the volumes of all these cases are constant.

The NaOH solutes reacted per second for all concentration of NaOH solutions are derived and shown in Table 2. From the table, when the concentration of NaOH solution is 15%, the NaOH solute reacted per second is the highest. Together with the gas absorption rates shown in Figure 10, considering both gas absorption rate and solute reaction rate, 15% of NaOH initial concentration is an optimal value.

Table 2 Solute reaction rate via initial NaOH concentrations

-- Insert Table 2 here --

5.2.2. Effect of gas flow rate on absorption rate

Three different gas flow rates (6.32×10^{-4} , 9.49×10^{-4} , 1.90×10^{-3} kg/s) are selected in the experiment to estimate the effect of gas flow rate on CO₂ absorption rate. Accordingly, three set of simulations are conducted with same flow rates to verify the applicability of CFD simulations. To predict the trend at higher gas flow rate, two more sets of gas flow rates (2.09×10^{-3} , 2.85×10^{-3} kg/s) were applied and tested in the CFD simulations. The results from the simulations and experiment are presented in Figure 12. Comparing with experiment results, simulation results are matching well when flow rates are 9.49×10^{-4} and 1.90×10^{-3} kg/s. The simulation result with flow rate of 2.09×10^{-3} kg/s is also well matched with the value of prediction based on experiment results. However, for the flow rates of 6.32×10^{-4} and 2.85×10^{-3} kg/s, the differences between experiment and simulation results cannot be neglected. It indicates the CFD model is not compatible with too low and too high gas flow rate.

-- Insert Figure 12 here --

Figure 12 Comparison of experimental and simulated gas absorption rate under different gas flow rate

From the simulation results shown in Figure 12, the percentage of gas absorbed is as high as 85% when gas flow rate is 6.32×10^{-4} kg/s. It is because the gas is fed into the solution slowly and can be absorbed more thoroughly. It

means the contact time between the gas and solution is more than other cases. However, in the experiment, the friction loss along from the flow meter to the diffuser impacts the actual gas flow rate. Due to the friction, the actual gas input flow rate into the reaction tank is smaller than the reading on flow meter. While the theoretical analyses are still using 6.32×10^{-4} kg/s from the reading of the flow meter, thus, the value of the gas flow rate used in analyses is larger than actual one. Therefore, it results in the calculated gas absorption rate for experiment is smaller than actual one.

With the flow rate of 2.85×10^{-3} kg/s, the gas input rate is the largest among all the cases. It results in the lowest absorption rate. This is because the contact time between the gas and the solution is too short at a high gas flow rate, leading to a low absorption rate.

-- Insert Figure 13 here --

Figure 13 Na₂CO₃ concentration over time for different gas input flow rates

Figure 13 presents CFD simulation results of the change of Na₂CO₃ mass fraction in the solution over time at different CO₂ gas feeding rates. It illustrates the time taken for the absorption process to reach to full reaction under different gas flow rates. The quantity of reacted NaOH solute per second under the set gas flow rates is considered in order to estimate the optimized gas flow rate for the maximum reaction rate. As the volume and concentration of NaOH solution is constant, the amount of NaOH solute in unit volume ([Eqs. 15](#)) is constant. Table 3 indicates a comparison of solute reaction rates at different flow rates. It is found the reaction rate is increased as the gas flow rate is increased. Combining Figure 12 and Figure 13, it shows a fact that a slow gas flow rate improves the absorption rate, but it takes a longer period to reach full reaction. Experiment and simulation results have shown a good agreement when the CO₂ gas flow is in the region of 9.49×10^{-4} to 2.09×10^{-3} kg/s. However, flow rate at the higher end of the region is preferred as it offers a higher reaction rate.

Table 3 Solute reaction rate under different gas input mass flow rates

-- Insert Table 3 here --

5.2.3. Impact of reaction tank geometry on gas absorption rate

The geometry parameters of reaction tank are factors that could impact the gas absorption rate significantly. This section discusses the results from simulation and experiment on how the geometry parameters affect the absorption reaction process. Three conditions are considered: change of solution column height under the same tank diameter, change of tank diameter with a constant solution column height and change of tank diameter with the same solution volume.

5.2.3.1. Impact of solution column height

To find out how the solution column height affects the absorption, a group of experiments is conducted with controlled diameter and variable column height. Figure 14 shows a comparison of experiment and simulation results and it indicates a good agreement between them. The maximum difference between the experiment and simulation results is 5.27%. The figure illustrates that with the same reaction tank diameter, an increase in the solution column height will bring a better gas absorption rate. The reason of this phenomenon is simply because the path of the gas in the solution is longer with the higher solution column, resulting longer contact time and good absorption.

-- Insert Figure 14 here --

Figure 14 CO₂ absorption rate for different solution column heights with a constant tank diameter

Figure 15 presents the simulation results of time spent of the three cases for a full reaction. It indicates that a low column height will have a fast reaction speed. At 30 cm column height, it takes almost 1100s to complete the reaction which it only costs 570s for the case with 10.5 cm column height. This can be explained that with same tank diameter, the quantity of solution with 30 cm column height is almost three times of that with 10.5 cm. According to the mass balance and reaction formula in [Eqs. 1](#), an increase in solution quantity directly leads an increase in CO₂ required for a complete reaction and therefore it increases the time of reaction.

-- Insert Figure 15 here --

Figure 15 Mass fraction of Na_2CO_3 over time for different solution column heights with controlled tank diameter

Quantity of NaOH solute reacted per second is considered here to find out the reaction rate under different solution column heights. Since the solution concentration is a constant, the mass of NaOH solute in unit volume of solution in [Eqs. 15](#) are constant. Then considering the reaction time in Figure 15, the mass of NaOH solute reacted per second in unit volume can be derived and presented in Table 4. However, the solution quantity (volume) is not constant at different solution column heights so a correction coefficient, ratio of solution column heights, is introduced. The mass of NaOH solute reacted per second (A') in Table 4 presents the corrected NaOH solute reaction rate. It indicates the reaction rate is higher with higher column height when tank diameter is a constant. Therefore, Figure 14 and Table 4 indicate that a high solution column height brings better gas absorption and a faster solute reaction. During system design, a longer contact period between gas and solution should be preferred.

Table 4 Solute reaction rate under different solution column heights with fixed tank diameter

-- Insert Table 4 here --

5.2.3.2. Impact of tank diameter with the same solution column height

This group of experiments has a condition of using the same solution column height but varying tank diameter. Figure 16 illustrates a comparison of simulation and experiment results. Again, a good agreement has been found between the experiment and simulation results. The difference between the simulation and experiment is minor which is no greater than 1.5%. In the figure, the gas absorption rate is to be increased when increasing the reaction tank diameter due to an increased contact area between the gas and solution. The gas fed into the reaction tank will not only move upward but also be diffused horizontally. The profile of gas distribution of gas is the same under all experiment conditions and the simulation due to the usage of the same diffuser. When height of solution column is a constant, the larger the diameter is, the wider the solution area is. Therefore, a large diameter of reaction tank leads to a good absorption rate of gas when the solution column height is a constant.

-- Insert Figure 16 here --

Figure 16 CO₂ absorption rates for different reaction tank diameters with controlled solution column height

According to Figure 17, the fastest reaction occurs with the tank of the smallest diameter due to less quantity of solution contained in a small diameter tank. The difference of reaction time amount the three cases vary from about 100s to 30s. Compared with effect of other geometric parameters, the impact of diameter on reaction rate speed is less when the solution column height is fixed. The mass of solute reacted is analyzed in order to find out the reaction rate varying with the diameter of reaction tank. Similar to Section 5.2.3.1, the concentration of the NaOH solution is a constant but the solution quantity is not constant. The mass of NaOH solute in unit volume is constant but the correction mass of NaOH solute reacted per second, A' , is used for analysis. Table 5 indicates that with same column height, large tank diameter will bring a fast reaction rate. Therefore, together with Figure 16, large tank diameter results both good gas absorption rate and quick reaction rate.

-- Insert Figure 17 here --

Figure 17 Mass fraction of Na₂CO₃ over time for different tank diameters with controlled solution column height

Table 5 Solute reaction rate under different tank diameters with fixed solution column height

-- Insert Table 5 here --

5.2.3.3. Impact of tank diameter with the same volume

Three sets of experiment are conducted at different tank diameter with a controlled solution volume. Figure 18 presents a comparison between experiment and simulation results. The difference values between the simulation and experiment results are about 2.88% max. The figure indicates the gas absorption rate decreases as the tank diameter increases. There are two factors that dominate this phenomenon: gas diffusion profile and gas path. Referring to section 5.2.3.2, the diffusion of gas will lead to a better gas absorption rate. However, with the same solution volume, a small tank diameter results high column height. Based on section 5.2.3.1, a high solution

column leads to a long gas path and long contact time between the gas and the solution. In this set of experiment and simulation, the effect of column height is dominating, so a smaller diameter of reaction tank leads to a better gas rate.

-- Insert Figure 18 here --

Figure 18 CO₂ absorption rates for different reaction tank diameters with controlled solution volume

Figure 19 illustrates the time cost obtained by the simulation for a complete reaction with different tank diameters. It indicates that small diameter leads to a fast reaction. The largest difference between the reaction times at different simulation conditions is about 100s. Since the concentration and quantity of solution is a constant, the mass of NaOH solute in unit volume is also a constant so that the reaction rate is inversely proportional to the reaction time. Therefore, when the solution quantity is fixed, a smaller diameter of reaction tank leads to both better gas absorption rate and a faster reaction rate.

-- Insert Figure 19 here --

Figure 19 Mass fraction of Na₂CO₃ over time for different tank diameters with controlled solution volume

5.2.4. Impact of operation temperature

Having evaluated the effect of gas input flow rate and geometry of tank on CO₂ absorption rate in section 5.2.2 and 5.2.3, the effect of environment conditions of experiment on the absorption rate is examined. According to [Eqs. 12](#), the environment temperature is one of the key factors affecting the reaction rate. In this section, the simulation results of absorption process under different environment temperatures will be presented. As the atmosphere condition will be changed from the assumption in Section 4.2, a new assumption is made that the gas initial temperature is 298K.

Figure 20 presents the simulation results under different environment temperature conditions. The range of temperature varies from 278 to 318K. Referring to Figure 20, the chemical reaction rate of the process is increasing as the temperature rises. According to [Eqs. 12](#), the chemical reaction rate is affected by temperature.

Due to heat exchange taking place between the atmosphere and the mixture of gas and solution, a high environment temperature leads to a high temperature of the mixture of gas and solution, resulting in a high reaction rate.

-- Insert Figure 20 here --

Figure 20 Simulated absorption rates under different operation temperatures

Figure 21 shows the time elapsed to reach full reaction at various environment temperatures. It is apparent that the fastest reaction happens when the environment temperature is 318K and the slowest one happens at 278K. The fastest reaction rate is 35 times of the slowest one. Hence, the environment temperature has a significant effect on the reaction speed and absorption rate. The results show that for the selected range of environment temperature, when the temperature is below 298K, the time taken for a full reaction is significantly high. Therefore the environment temperature onboard ship for the system's operation should be maintained above 298K.

-- Insert Figure 21 here --

Figure 21 Na₂CO₃ concentrations over time for different operation temperatures

6. Conclusions and further studies

This paper demonstrates a feasibility of using carbon solidification method for CO₂ emission reduction from by ships experiment and computer numerical simulation. It illustrates the simulation results have an acceptable agreement with that of the experiment. This indicates the simulation model developed can be utilized as a fundamental tool for design and scale up of real systems on ship. A series of investigation have been carried out on factors which have significant effect on carbon absorption process. Conclusions have been reached that 15% mass fraction of NaOH solution offers the optimal gas absorption rate; a low CO₂ gas flow rate could lead to a high absorption rate in a specific region, from 9.49×10^{-4} to 2.09×10^{-3} kg/s. Results from both experiment and simulation also prove that a good contact between gas and solution will lead to a better absorption; the absorption

reaction benefits greatly from a high temperature of solution. A good contact between gas and solution can be achieved by optimizing the three geometry factors, i.e. tank diameter, solution volume and solution height. CO₂ gas flow rate is also an important parameter affecting the contact between gas and solution.

For future study, a proto-type of the absorption system will be designed by making use of the models developed in the research. The model is accurate enough to simulate of real scale system. With availability of funding, a real system will be designed and installed as an onboard in-line system for a case ship which will cover the absorption of CO₂ by solution, precipitation of CO₃²⁻ and the storage of final product.

Acknowledgment

We are grateful to the Scottish Environmental Technology Network for providing laboratory facilities. Simulations results were obtained using the EPSRC funded ARCHIE-WeSt High Performance Computer (www.archie-west.ac.uk). EPSRC grant no. EP/K000586/1. Authors appreciate the financial supports on the project from the Department of Naval Architecture and Marine Engineering of University of Strathclyde.

References

- ANSYS Fluent 14.5, Theory Guide, 2012, USA. <http://www.ansys.com>
- Asendrych, D., Niegodajew, P., Drobniak, S., 2013. CFD Modelling of CO₂ Capture in a Packed Bed by Chemical Absorption. *Chemical and Process Engineering*, 34(2), pp. 269-282. Retrieved 17 Oct. 2014, from doi:10.2478/cpe-2013-0022. <http://www.degruyter.com/view/j/cpe.2013.34.issue-2/cpe-2013-0022/cpe-2013-0022.xml>
- Boundary Dam Integrated Carbon Capture and Storage Demonstration Project, SASKPOWER CCS, Canada, 2014. http://www.saskpower.com/wp-content/uploads/clean_coal_information_sheet.pdf
- Chambers, C., Holliday, A.K., 1975. *Modern inorganic chemistry-An intermediate text*, Butterworth & Co (Publishers) Ltd 1975, 133pp. <http://files.rushim.ru/books/neorganika/Chambers.pdf>.
- DNV and PSE report on ship carbon capture & storage, Det Norske Veritas, Oslo and London, 2013, http://www.psenderprise.com/news/data/130211_dnv_ccs.pdf.
- FutureGen 2.0 Project, Final Environmental Impact Statement, U.S. Department of Energy, USA, October, 2013. http://energy.gov/sites/prod/files/2013/10/f4/EIS-0460-FEIS-Volume_II_Part_1-2013.pdf
- Global CCS Institute 2012, the Global Status of CCS: 2012, Canberra, Australia. ISBN 978-0-9871863-1-7. <http://decarboni.se/sites/default/files/publications/47936/global-status-ccs-2012.pdf>

- Gorgon Carbon Dioxide Injection Project, Chevron Australia, Australia, 2015.
<http://www.chevronaustralia.com/docs/default-source/default-document-library/fact-sheet-gorgon-c02-injection-project.pdf?sfvrsn=8>
- Hessabi M., 2009. An Overview of Lime Slaking and Factors that Affect the Process, Chemco Systems, L.P.
http://chemcoequipment.com/Files/Admin/Publications/AN_OVERVIEW_OF_LIME_SLAKING.pdf
- Horvath, A, Jordan, C., Lukasser, M., Kuttner, C., Makaruk, A., Harasek, M., 2009, CFD Simulation of Bubble Columns using the VOF Model: Comparison of commercial and Open Source Solvers with an Experiment, Chemical Engineering Transactions, Volume 18 (2009), DOI: 10.3303/CET0918098.
<http://www.aidic.it/cet/09/18/098.pdf>.
- IPCC, 2007: IPCC Special Report on Carbon Dioxide Capture and Storage. Prepared by Working Group III of the Intergovernmental Panel on Climate Change [Metz, B., O. Davidson, H. C. de Coninck, M. Loos, and L. A. Meyer (eds.)]. Cambridge University Press, Cambridge, United Kingdom and New York, NY, USA, 442 pp.
- Jiyuan, T., Guan-Heng, Y.,Chaoqun, L., Chapter 6 - Practical Guidelines for CFD Simulation and Analysis, In Computational Fluid Dynamics (Second Edition), edited by Jiyuan TuGuan-Heng YeohChaoqun Liu, Butterworth-Heinemann, 2013, Pages 219-273, ISBN 9780080982434, <http://dx.doi.org/10.1016/B978-0-08-098243-4.00006-8>.
- Mahmoudkhani, M., Keith, D.W., 2009. Low-energy sodium hydroxide recovery for CO₂ capture from atmospheric air—Thermodynamic analysis, Energy and Environmental System Group, Institute for Sustainable Energy, Environment, Economy, University of Calgary, Canada.
- MARPOL Annex VI, Chapter IV, MEPC, 2011.
- Mohammad, I., Mohammad, A.K., 2011. Investigation of Bubble Column Hydrodynamics Using CFD Simulation (2d and 3d) and Experimental Validation, Petroleum and Coal 53 (2) 146-158 (2011),
http://www.vurup.sk/sites/default/files/downloads/pc_2_2001_irani_111.pdf
- Peilin, Z, Haibin, W, 2014. Carbon capture and storage— Solidification and storage of carbon dioxide captured on ships, Ocean Engineering 91 (2014) 172–180, <http://dx.doi.org/10.1016/j.oceaneng.2014.09.006>.
- Pflug, I.J., Angelini, P., Dewey, D.H., 1957. Fundamentals of Carbon Dioxide Absorption as They Apply to Controlled-atmosphere Storage, Department of Agricultural Engineering and Horticulture.
- Shipping, World Trade and the Reduction of CO₂ Emissions, United Nations Framework Convention on Climate Change (UNFCCC), International Chamber of Shipping (ICS), Representing the Global Shipping Industry, London, UK, 2014. <http://www.ics-shipping.org/docs/default-source/resources/environmental-protection/shipping-world-trade-and-the-reduction-of-co2-emissions.pdf?sfvrsn=6>.
- Third IMO GHG Study 2014, International Maritime Organization, Suffolk, United Kingdom, April, 2014.
<http://www.imo.org/en/OurWork/Environment/PollutionPrevention/AirPollution/Documents/Third%20Greenhouse%20Gas%20Study/GHG3%20Executive%20Summary%20and%20Report.pdf>
- World Resources Institute (WRI). CCS Guidelines: Guidelines for Carbon Dioxide Capture, Transport, and Storage. Washington, DC: WRI, 2008. ISBN 978-1-56973-701-9. http://pdf.wri.org/ccs_guidelines.pdf